Journal of Non-Crystalline Solids 429 (2015) 98–103

Contents lists available at ScienceDirect

Journal of Non-Crystalline Solids

journal homepage: www.elsevier.com/ locate/ jnoncrysol

Glass transition of aluminum melt. Molecular dynamics study

L.N. Kolotova [a,b,*], G.E. Norman [a,b], V.V. Pisarev [a,b]

[a] Moscow Institute of Physics and Technology (State University), Dolgoprudny 141700, Russia
[b] Joint Institute for High Temperatures, Russian Academy of Sciences, Moscow 125412, Russia

ARTICLE INFO

Article history:
Received 9 July 2015
Received in revised form 15 August 2015
Accepted 21 August 2015
Available online xxxx

Keywords:
Glass transition;
Molecular dynamics;
Icosahedra;
Self-diffusion;
Heat capacity;
Radial distribution function;
Aluminum

ABSTRACT

Molecular dynamics study of transition from liquid aluminum into an amorphous state is carried out. Different criteria for the glass transition are compared with each other: splitting of the second peak of the radial distribution function, increasing of the number of atoms with icosahedron-like environment, increase of the self-diffusion activation energy, changes in the heat capacity. The discrepancy of the results obtained by different criteria is discovered. Heat capacity dependence on temperature agrees qualitatively with theoretical and experimental results. Influence of cooling rate on the glass transition temperature is studied. Although different methods give different glass transition temperatures, the dependencies on cooling rate may be interpreted in the Volkenstein and Ptitsyn's framework using either Arrhenius or Vogel–Fulcher–Tammann relaxation laws.

1. Introduction

Amorphous metals have a unique non-crystalline structure. Because of this, they have physical and magnetic properties combining strength and rigidity with the flexibility and toughness which are unusual for polycrystalline solids. It is known that there is a strong dependence of the structure and properties of glasses on the conditions and methods of manufacturing [1–8]. The main problem of the physics of liquid-glass transition is how to distinguish these two noncrystalline phases clearly [9–13]. There is no generally accepted theory describing the details of the glass transition. A large variety of experimental data, corresponding to different laws for different matters, leads to a large number of theories. For example, the glass transition in [6,7,14] is considered in the approximation of mode-coupling theory in the system described by a form of repulsive shoulder potential of solid spheres. This transition is associated with changes of some "order parameter" in [1,2,4,5].

Glass transitions and phase transition have a lot in common. Many properties of material such as the specific heat, compressibility and viscosity undergo a sharp change in a narrow temperature range. Nevertheless, despite some similarity, the glass transition is not a phase transition in a strict sense. Thus, one can obtain glasses with different internal structure at different cooling rates.

Transition is not accompanied by sharp symmetry change at the molecular level as in the case of the liquid-crystal transition. Both experiments and atomistic simulations for a number of substances confirm that the second peak of the radial distribution function (RDF) begins splitting when the melt viscosity undergoes a sharp change [9]. So, splitting of the second peak of RDF can be used as a criterion for the glass transition.

The molecular dynamics (MD) method allows us to describe physical processes on the atomistic level. One can perform a detailed study of glass and phase transitions and obtain different characteristics of this process [15–21]. RDF is usually used in MD simulations for analysis of the amorphous structure and determining the glass transition. Voronoi polyhedra are used for a more detailed examination of the structure [22,23]. Influence of the number of different types of Voronoi polyhedra on the form of pair correlation functions second peak is considered in [9].

In this paper, glass transition of aluminum melt during isobaric cooling is considered using the MD method. In Section 2, the calculation technique is described. Structural and dynamic criteria for the glass transition are compared with each other in Section 3. Calorimetric criteria for calculation of glass transition temperature on cooling and re-heating are considered in Section 4. Influence of cooling rate on the glass transition temperature is studied in Section 5. Conclusions follow in Section 6

* Corresponding author at: Moscow Institute of Physics and Technology (State University), Dolgoprudny 141700, Russia.
E-mail address: lada.kolotova@gmail.com (L.N. Kolotova).

http://dx.doi.org/10.1016/j.jnoncrysol.2015.08.025
0022-3093/

2. Molecular dynamics model

Aluminum melt cooling is taken as an example to study a glass transition. Liquid aluminum is described by a many-body embedded atom method potential [24]. The potential energy of the system in this approach is represented as follows:

$$U = \sum_{i<j} \varphi(r_{ij}) + \sum_j F(\overline{\rho}_j), \overline{\rho}_j = \sum_{j \neq i} \rho(r_{ij}). \quad (1)$$

The first term is a sum of pair potentials φ over all atom pairs in the system, r_{ij} is the distance between atoms i and j. A non-linear embedding function $F(\rho)$ introduces many-body effects. $\bar{\rho}$ is an effective electron density that is induced by the neighboring atoms at the given atom and $\rho(r_{ij})$ is a contribution from each neighbor. The parametrization of the potential is suggested in [25].

Molecular dynamics method [18,26] is used to study the aluminum melt. Simulations are performed using the LAMMPS MD software [27]. Numerical integration of the equations of motion is done using 1 fs timestep.

To create the initial configuration, atoms are placed at the sites of the fcc lattice with parameter $a_0 = 4.08$ Å. A simulation box $40a_0 \times 20a_0 \times 20a_0$ along the axes x, y, z with the periodic boundary conditions on all axes is used. 32,800 atoms are placed as a thin film which takes half of the volume of the simulation box ($x \geq 20a_0$).

Free space in the simulation box allows the film to change its thickness during the cooling process. That is why the atoms are able to occupy a volume corresponding to a constant near-zero pressure. Therefore, no additional barostat is necessary to apply to maintain the isobaric conditions during cooling or heating processes. This is similar to the real conditions.

At the initial step, random (in magnitude and direction) velocities are given to all the atoms. They are normalized so that the kinetic energy of the atoms corresponds to the temperature $T = 2000$ K. A crystal melting process is carried out at 2000 K for the first 900 ps. Then, the system is cooled down to 1500 K and additional equilibration at this temperature takes place.

The temperature of the system is changed by the following procedure. First, we choose a cooling rate and calculate the desired linear dependence of temperature on time. The time integration is then performed using the conventional velocity Verlet scheme. The velocities of atoms are rescaled every 100 fs to match the chosen dependence of temperature on time. This method allows us to avoid unphysical temperature oscillations characteristic to the Nose-Hoover thermostat with the rapidly changing target temperature.

For the study of the glass transition, rapid cooling of melt from 1500 K to 300 K is carried out at constant rates. MD simulations are performed for cooling rates from 10^{10} K/s to 10^{13} K/s.

3. Criteria for the glass transition

Two structural criteria and a dynamical one are considered in this section. Changes in the RDF, number of icosahedral clusters and self-diffusion coefficient are monitored during the cooling.

The procedure is repeated for a number of cooling rates. The results are presented below for the rate $|dT/dt| = 10^{13}$ K/s[1] as an example. They are typical for the all cooling rates considered.

3.1. Splitting of the second peak of RDF

The well-known criterion is splitting of RDF's peak in the second coordination sphere. It corresponds to the appearance of two local maxima and a local minimum between them. This is equivalent to the existence of r_0, for which $G(r_0 \pm h) - G(r_0) > 0$, where $G(r)$ is the RDF and h is the spatial step the RDF is calculated with.

The area S enclosed between the tangent drawn at the point r_0 to the graph of RDF and the graph of RDF itself in the second coordination sphere is used as the mathematical measure of peak splitting (Fig. 1):

$$S = \int_{r_1}^{r_2} (G(r) - G(r_0))dr \quad (2)$$

where r_1 and r_2 are determined from the condition $G(r_{1,2}) = G(r_0)$. There are no such points when RDF is far from splitting, and thus the integral in Eq. (2) reduces to zero for the liquid state.

The results are presented for the whole temperature range in Fig. 2a. The range of the glass transition reveals itself about 900 K.

3.2. Number of icosahedral clusters

Extremely supercooled metallic melts of one-component systems are characterized by an icosahedral short-range order [28,29,30,31]. Recently more and more papers are devoted to the description of metallic glass structure through the packaging of clusters with different local order [32,33,34]. In particular, the 13-atom icosahedral clusters are proposed as a structural unit responsible for the formation of metallic glasses [13,35,36]. Recently their existence in metallic glasses were confirmed experimentally for $Zr_{36}Cu_{64}$ alloy [13] by X-ray scattering. However, it is also shown that not all metal alloys demonstrate increase of number of such clusters at glass transition.

Analysis of the number of icosahedral cluster is carried out at the aluminum melt cooling in this paper. Common Neighbor Analysis (CNA) [37] is used to identify them. This method is also used for identifying crystal lattice short-range order during crystallization. Atom with its nearest neighbors corresponding to the fist peak of RDF forms "bonded" pairs. These bonds are classified by the combination of 3 indexes *jkl*. The first index, *j*, is the number of neighbors common to both atoms. The second index, *k*, is the number of bonds between these common neighbors. The third index, *l*, is the number of bonds in the longest continuous chain formed by *k* bonds between common neighbors. After it, different types of bonds are associated with different local order. Icosahedral order is characterized by 555 bonds. Number of atoms participating in twelve 555 bonds is thought of as the number of icosahedral clusters N_{ic}.

There are no icosahedral clusters at high temperatures or their quantity differs insignificantly from zero. However, N_{ic} begins to increase

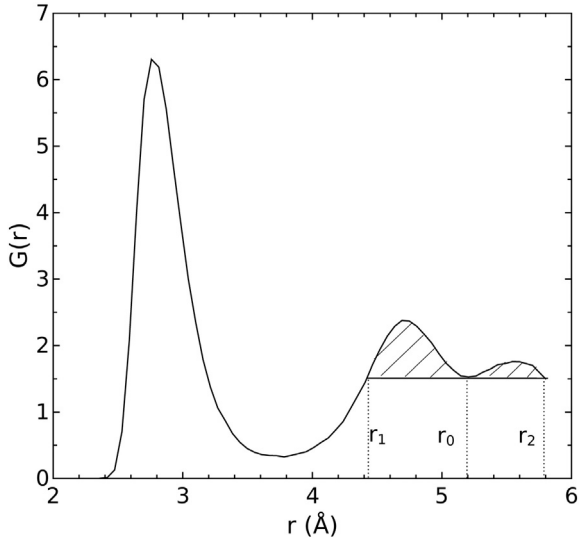

Fig. 1. Splitting of the second peak of radial distribution function. r_0 is determined from the Eq. (2), $r_{1,2}$ satisfy the condition: $G(r_{1,2}) = G(r_0)$.

[1] We will further use absolute values of temperature change rate, the rate itself is negative in the cooling process and positive in the re-heating process.

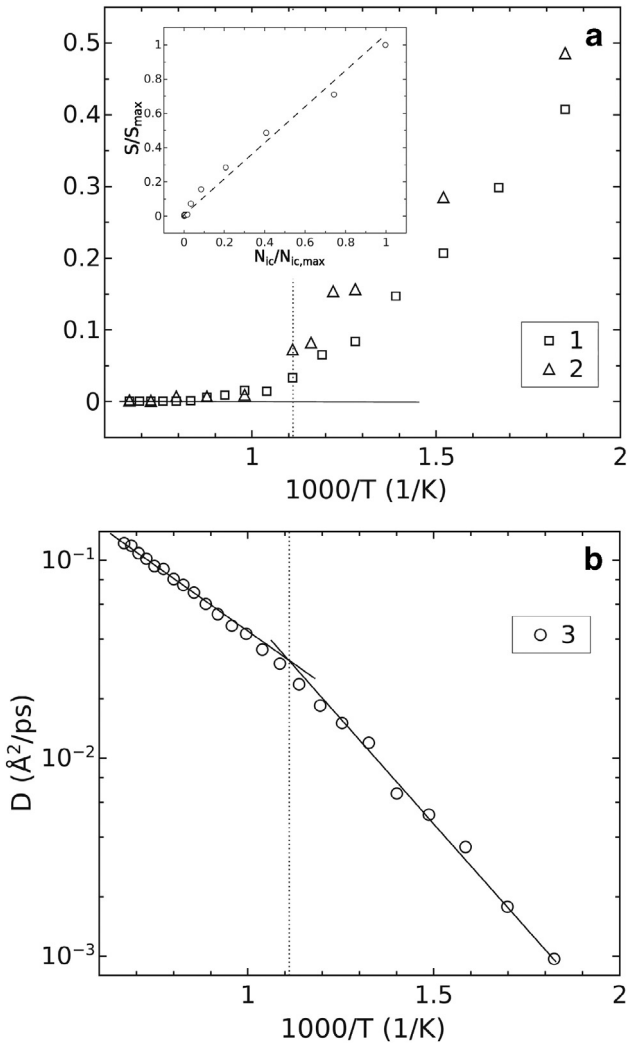

Fig. 2. (a) Dependences of the fraction of icosahedral clusters $N_{ic}/N_{ic,\max}$ (1) and degree of peak splitting $S/S_{\max}$ (2) on temperature. $S_{\max}$ and $N_{ic,\max}$ are the values at 300 K. Inset: correlation between the peak spliting and the number of icosahedral clusters. Linear correlation is shown for the comparison. (b) Self-diffusion coefficient dependence on temperature (3). $|dT/dt| = 10^{13}$ K/s. Vertical lines on (a) and (b) denote the glass transition temperature.

sharply when the melt is cooled (Fig. 2a). The range of increase coincides with the temperature range of the glass transition revealed for *S*. Furthermore, the degree of second peak splitting correlates with the fraction of icosahedra in the system (inset on Fig. 2a).

3.3. Change in the activation energy of self-diffusion of atoms

Another characteristic of the glass formation is a decrease in mobility of atoms. This reflects in the change of the self-diffusion coefficient *D* of atoms. The value of *D* can be obtained from the Einstein-Smoluchowski equation

$$\overline{\Delta r^2} = 6Dt \tag{3}$$

where $\overline{\Delta r^2}$ is mean square displacement of atoms from the initial position for the time *t*.

In this paper, self-diffusion coefficient is evaluated from equilibrium MD trajectories at constant temperature using Eq. (3). Successive atomic configurations are saved during the cooling process of the melt from 1500 K to 300 K. Such configurations are chosen every 40 K outside the glass transition range estimated from RDF peak splitting and every 4 K inside it. Each configuration is used then as the initial configuration for the equilibrium MD run.

The increase of the slope of the curve in the coordinates $\lg D$-$1/T$ takes place in the temperature range of the glass transition (Fig. 2b). The self-diffusion activation energy changes from 0.26 eV to 0.42 eV during the glass transition. The value of 0.42 eV for temperatures below 900 K is a conditional one, since it continues increasing for temperatures below 700 K.

A sharp increase in the number of atoms with icosahedral environment and splitting of the second peak of the pair correlation function are usually considered to be structural glass transition criteria. They are also accompanied by an increase in the activation energy of self-diffusion. Results in Fig. 2 show that three criteria are equivalent to each other with respect to the location of the glass transition range. Therefore it is possible to use any of them. The splitting of the second peak RDF is the simplest and most straightforwardly calculated criterion.

4. Calorimetric criteria

Changes in heat capacity during cooling or heating are the most convenient and commonly used criteria for determining the glass transition temperature in the experiments [38,39]. The heat capacity can be calculated from the MD simulations as well using the obvious expression

$$C_p = \delta H/\delta T \tag{4}$$

where $H = U + PV$. Pressure $P \approx 0$ at normal conditions, so $H \approx U$. Internal energy *U* is calculated straightforwardly in the MD simulations. The $H(T)$ dependencies are calculated for each cooling rate at constant zero pressure. The calculations are repeated for 30 initial configurations. These configurations differ from each other only by the realization of the initial velocity distribution of atoms at 2000 K. The results are averaged over these 30 MD runs. Averaging is necessary to obtain a smooth enough function for its subsequent numerical differentiation.

The same procedure is performed for the re-heating process. Re-heating rate is equal to the cooling rate for each state.

Fluctuations of the heat capacity obtained by numerical differentiation are significant, even when MD runs are averaged over 30 initial configurations. Therefore, the low pass Fourier filter is used to cut out the frequencies above 0.05 K^{-1}. 95% of the signal power is located within the frequency range used. The Fourier filter permits to smoothen dependencies of heat capacity on temperature.

Glass is a non-equilibrium state. One of the signs of it is a pronounced hysteresis in the heat capacity: the heat capacity C_P dependencies on temperature under cooling and under re-heating of glass are different. The $C_p(T)$ dependencies obtained in our simulations during re-heating show the characteristic “hump” of the heat capacity, whereas the heat capacity under cooling decreases smoothly during the entire process (Fig. 3).

Hump and hysteresis existence are known for many glasses from experiments [38,39,40,41]. One of the explanations to such behavior of the heat capacity of glasses is proposed in [1,2,4,5] on the basis of a “order parameter” relaxation.

The $C_P(T)$ dependence for aluminum glass calculated from MD simulations agrees with the experimental data for polymer glasses by Zhurkov and Levin [40] up to the shift and scaling of the coordinates (Fig. 4). Such correspondence implies similarities in the glass transition underlying mechanisms for metals and polymers.

There is no clearly defined glass transition temperature T_g, in contrast to the phase transitions. Even for the calorimetric determination of T_g, there are several methods [39]. The easiest one is to define it as the temperature at which the heat capacity during cooling is reduced by half of the total change in the whole vitrification process.

Another criterion employs the so-called “fictive temperature” T_f [39]. The fictive temperature which can be measured in the re-heating

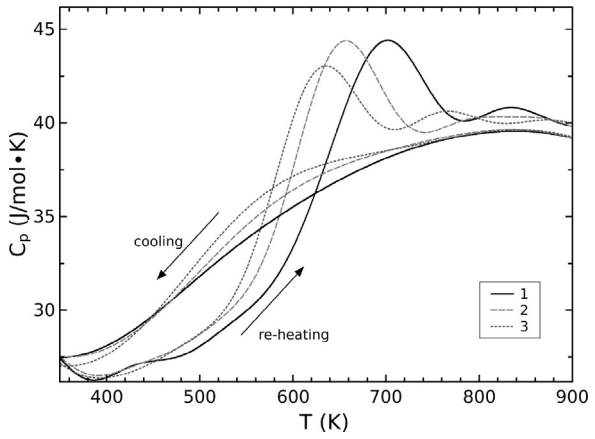

Fig. 3. Heat capacity dependencies on temperature. $|dT/dt|$ is equal to $2 \cdot 10^{12}$ K/s (1), $1.3 \cdot 10^{12}$ K/s (2), $6 \cdot 10^{11}$ K/s (3).

process and is often thought to be the same, or close to, the glass transition temperature T_g. The value of T_f is determined from the following condition — enthalpy change during melting of the glass on re-heating is equal to enthalpy change as if the glass-liquid transition occurred instantly at the temperature T_f (Fig. 5).

5. Glass transition temperature dependence on cooling rate

To define these dependencies we follow the Volkenstein and Ptitsyn's approach [2,42,43,44] where the dependence of T_g on cooling rate at constant pressure is derived from the criterion:

$$|dT/dt|\tau = const \text{ at } T = T_g \tag{5}$$

where τ is a relaxation time, $|dT/dt|$ is a cooling rate. Assuming Arrhenius dependence for relaxation time $\tau = \tau_0 \exp(U_0/kT)$, one can obtain the Bartenev equation after some transformations

$$1/T_g = C - k/U_0 \log|dT/dt| \tag{6}$$

Glass transition temperatures are calculated by using all of the criteria previously discussed. Dependencies T_g on $|dT/dt|$ are shown in Fig. 6 obtained by MD modeling for different glass transition criteria.

Calorimetric glass transition temperature and fictive temperature dependencies satisfy Eq. (6) with $U_0 = 0.5$ eV for the T_g and 1 eV for the T_f (Fig. 6a). The temperatures T_g and T_f turn out to be different. The

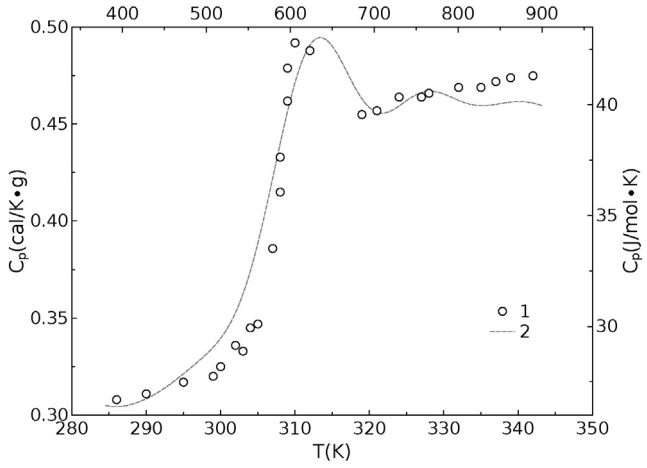

Fig. 4. Qualitative comparison of heat capacities at the re-heating of polymer glass (1, bottom and left axes) (Ref. [40]) and of aluminum glass (2, top and right axes) (current work).

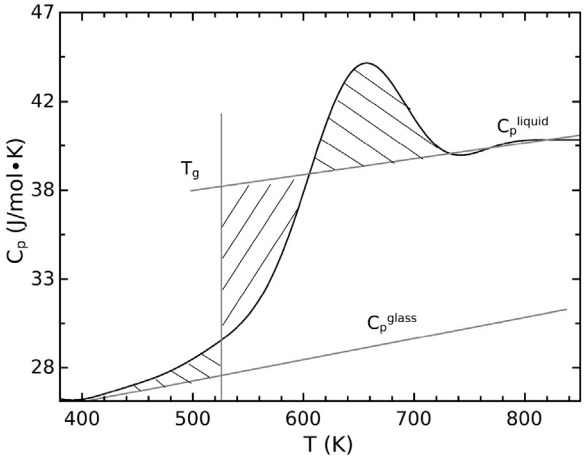

Fig. 5. The determination of fictive glass transition temperature from the heat capacity dependence on temperature. Enthalpy change during the glass melting is equal to enthalpy change as if the glass-liquid transition occurred instantly at this temperature.

discrepancy highlights the non-equilibrium nature of the glass formation and melting.

Structural (and dynamic) glass transition temperature shows divergence from Eq. (6) (Fig. 6). Strictly speaking, Fig. 6b shows two temperature ranges which fit approximately Eq. (6) but with different values of $U_0 = 4$ eV below 400 K and 40 eV above 400 K.

Fitting to straight lines is not accurate enough in Fig. 6b. Another attempt to fit the results of the structural (and dynamic) glass transition temperature to the alternative theory is presented in Fig. 6c. The character of the glass transition temperature dependence can be explained using non-Arrhenius relaxation [3]. The Vogel–Fulcher–Tammann (VFT) relaxation model $\tau = \tau_0 \exp[U_0/k(T\text{-}T^*)]$ with $U_0 = 0.013$ eV and $T^* = 805$ K gives an agreement with the simulation results (Fig. 6c) within the MD accuracy.

Only one of a number of glass transition criteria is usually considered in papers. RDF is usually used to characterize the structure of quenched glasses, and calorimetric method is convenient to use to determine glass transition temperature experimentally. In the current paper, two structural criteria, one dynamic criterion and two calorimetric criteria for glass transition are compared with each other.

Structural and dynamic criteria are equivalent with respect to the position location of the glass formation range (Fig. 2). Splitting of the second peak of the pair correlation function and sharp increase in the activation energy of self-diffusion and the number of atoms with icosahedral environment take place at the isobaric cooling of Al melt at temperatures higher than the calorimetric glass transition temperature. The appearance of a small amount of icosahedral clusters does not affect thermodynamic properties. But it leads to a marked drop in self-diffusion coefficient, and hence to a decrease in mobility. Differences between structural and calorimetric glass transition temperatures are also reported by other authors [45].

Only a weak dependence of the glass transition temperature on cooling rate is evident from Fig. 6. Thus, the curves may be extrapolated with reasonable accuracy up to the cooling rates ~10^9 K/s to obtain glass transition temperatures in the experimentally attainable range. 10^9 K/s is the estimated critical cooling rate for aluminum, following the approach given in [46].

6. Conclusions

MD simulations are performed for glass transition of supercooled aluminum melt at constant pressure. Structural, dynamic and calorimetric glass transition temperatures are calculated and compared with each other.

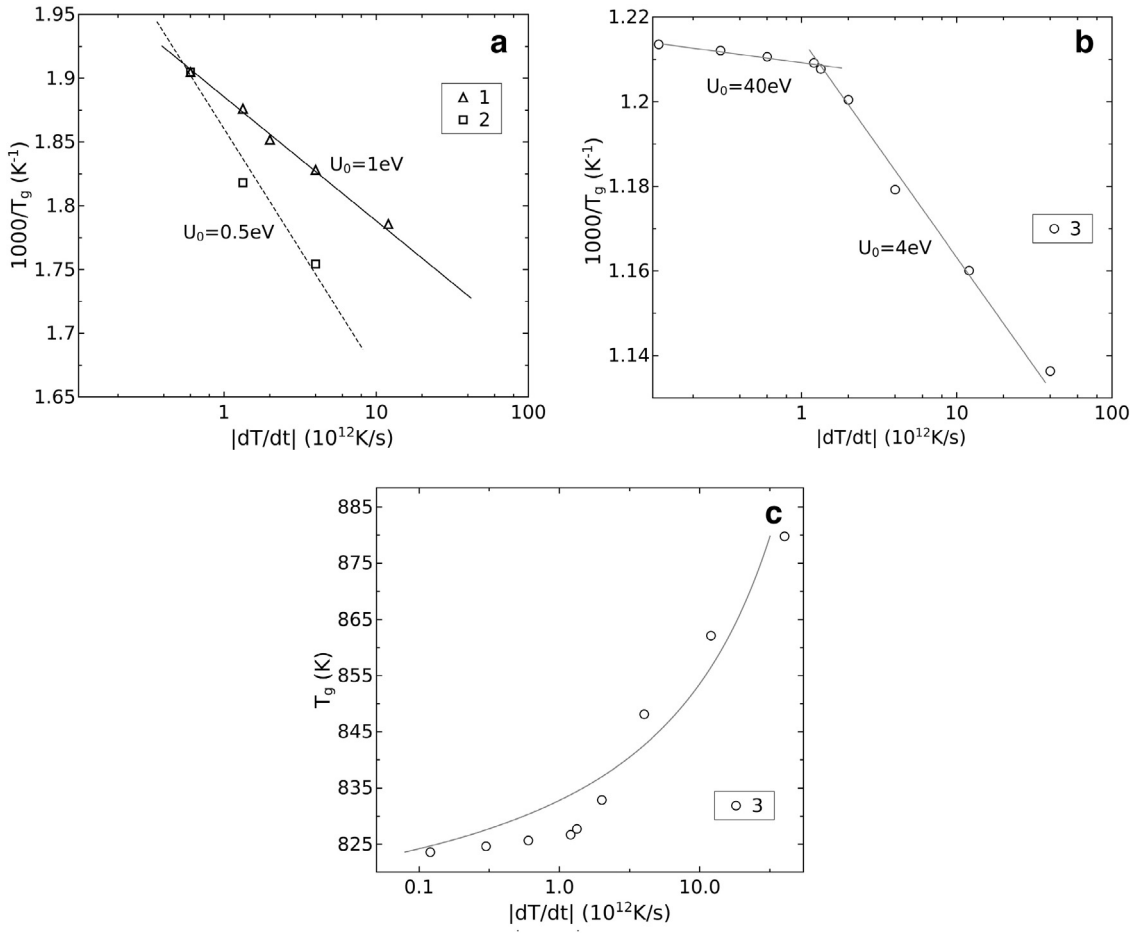

Fig. 6. Glass transition temperature dependence on cooling rate. (a) Fictive glass transition temperature (1) and calorimetric glass transition temperature (2). (b) Structural glass transition temperature. Solid lines show approximation by the Bartenev equation. (c) Structural glass transition temperature. Solid line shows the approximation using the VFT relaxation law.

The "structural" glass transition temperatures calculated using the RDF's second peak splitting as the criterion coincide with the "dynamic" glass transition temperature calculated using the self diffusion coefficient dependence on temperature. Furthermore, splitting of the second peak of the radial distribution function follows almost linearly the icosahedral clusters number.

The heat capacity is calculated during the glass transition and melting using MD method. Its dependence on temperature shows pronounced hysteresis and a characteristic "hump" at the re-heating. These features agree qualitatively with the experimental data and are a sign of a non-equilibrium glassy state.

The values of glass transition temperature from the calorimetric criterion are lower than the ones from the structural criteria. Moreover, the fictive temperatures calculated from re-heating simulations differ from glass transition temperatures. This implies that great care must be taken in choosing the criterion for the glass transition.

The dependence of the calorimetric glass transition temperature and fictive temperature on cooling rate may be described by the Bartenev equation. The dependence of the structural glass transition temperature, however, does not seem to follow this equation. Instead, the results on the structural glass transition temperature can be interpreted in terms of the Vogel-Fulcher-Tammann relaxation model.

Acknowledgments

The calculations were carried out on the MVS-100 K and MVS-10P clusters of the Joint Supercomputer Center of RAS, "Lomonosov" cluster of the Moscow State University. The work was partially supported by the RFBR grant no. 14-08-31587 mol_a (L.N. Kolotova, V.V. Pisarev), the Program for Basic Research of the RAS No. 43 "Fundamental Problems of Mathematical Modeling" (coordinator is ac. V.B. Betelin) and the President RF Scholarship SP-7488.2013.2 (V.V. Pisarev). Authors are grateful to Jürn W.P. Schmelzer and Timur Tropin for the helpful discussions.

References

[1] J.W.P. Schmelzer, E.D. Zanotto, V.M. Fokin, Pressure dependence of viscosity, J. Chem. Phys. 122 (7) (2005) 074511, http://dx.doi.org/10.1063/1.1851510 (URL http://www.ncbi.nlm.nih.gov/pubmed/15743258).
[2] J.W.P. Schmelzer, Kinetic criteria of glass formation and the pressure dependence of the glass transition temperature, J. Chem. Phys. 136 (7) (2012) 074512, http://dx.doi.org/10.1063/1.3685510 (URL http://www.ncbi.nlm.nih.gov/pubmed/22360253).
[3] J.W. Schmelzer, T.V. Tropin, Dependence of the width of the glass transition interval on cooling and heating rates, J. Chem. Phys. 138 (3) (2013) 034507.
[4] T.V. Tropin, J.W. Schmelzer, C. Schick, On the dependence of the properties of glasses on cooling and heating rates, J. Non-Cryst. Solids 357 (4) (2011) 1291–1302, http://dx.doi.org/10.1016/j.jnoncrysol.2010.11.111 (URL http://linkinghub.elsevier.com/retrieve/pii/S002230931000966X).
[5] T.V. Tropin, J.W.P. Schmelzer, I. Gutzow, C. Schick, On the theoretical determination of the Prigogine–Defay ratio in glass transition, J. Chem. Phys. 136 (12) (2012) 124502, http://dx.doi.org/10.1063/1.3694531 URL http://www.ncbi.nlm.nih.gov/pubmed/22462869).
[6] Y.D. Fomin, N.V. Gribova, V.N. Ryzhov, S.M. Stishov, D. Frenkel, Quasibinary amorphous phase in a three-dimensional system of particles with repulsive-shoulder interactions, J. Chem. Phys. 129 (6) (2008) 064512, http://dx.doi.org/10.1063/1.2965880 (URL http://www.ncbi.nlm.nih.gov/pubmed/18715090).
[7] V.N. Ryzhov, S.M. Stishov, Repulsive step potential: a model for a liquid–liquid phase transition, Phys. Rev. E 67 (1) (2003) 010201, http://dx.doi.org/10.1103/PhysRevE.67.010201.

[8] T. Chakrabarty, A.V. Mahajan, S. Kundu, Cluster spin glass behavior in geometrically frustrated $Zn_3V_3O_8$, J. Phys. Condens. Matter 26 (40) (2014) 405601 (URL http://stacks.iop.org/0953-8984/26/i=40/a=405601).
[9] S.P. Pan, J.Y. Qin, W.M. Wang, T.K. Gu, Origin of splitting of the second peak in the pair-distribution function for metallic glasses, Phys. Rev. B 84 (9) (2011) 1–4, http://dx.doi.org/10.1103/PhysRevB.84.092201.
[10] A. Fedorchenko, A. Chernov, Simulation of the microstructure of a thin metal layer quenched from a liquid state, Heat Mass Transf. 46 (5) (2003) 921–929, http://dx.doi.org/10.1016/S0017-9310(02)00350–2 (URL http://linkinghub.elsevier.com/retrieve/pii/S0017931002003502).
[11] V.A. Khonik, K. Kitagawa, H. Morii, On the determination of the crystallization activation energy of metallic glasses, J. Appl. Phys. 87 (12) (2000) 8440, http://dx.doi.org/10.1063/1.373560 (URL http://scitation.aip.org/content/aip/journal/jap/87/12/10.1063/1.373560).
[12] M. Mendelev, J. Schmalian, C. Wang, J. Morris, K. Ho, Interface mobility and the liquid-glass transition in a one-component system described by an embedded atom method potential, Phys. Rev. B 74 (10) (2006) 104206, http://dx.doi.org/10.1103/PhysRevB.74.104206.
[13] A.C.Y. Liu, M.J. Neish, G. Stokol, G.A. Buckley, L.A. Smillie, M.D. de Jonge, R.T. Ott, M.J. Kramer, L. Bourgeois, Systematic mapping of icosahedral short-range order in a melt-spun $Zr_{36}Cu_{64}$ metallic glass, Phys. Rev. Lett. 110 (20) (2013) 205505 (URL http://link.aps.org/doi/10.1103/PhysRevLett.110.205505).
[14] Y.D. Fomin, V.N. Ryzhov, V.V. Brazhkin, Properties of liquid iron along the melting line up to earth-core pressures, J. Phys. Condens. Matter 25 (28) (2013) 285104.
[15] W. Polak, Structural properties of solid nuclei forming in Lennard–Jones clusters during simulated cooling, Comp. Theor. Chem. 1021 (2013) 268–274.
[16] W. Polak, Formation of regular polyicosahedral and defected crystalline structures in growing Lennard–Jones clusters, J. Cryst. Growth 401 (2014) 44–50.
[17] A.Y. Kuksin, I. Morozov, G. Norman, V. Stegailov, I. Valuev, Standards for molecular dynamics modelling and simulation of relaxation, Mol. Simul. 31 (14–15) (2005) 1005–1017.
[18] G.E. Norman, V.V. Stegailov, Stochastic theory of the classical molecular dynamics method, Math. Models Comput. Simul. 5 (4) (2013) 305–333.
[19] D. Belashchenko, O. Ostrovskii, A molecular dynamics study of nickel crystallization at strong supercoolings, Russ. J. Phys. Chem. A 82 (3) (2008) 364–375.
[20] D. Belashchenko, Account for electron contributions in embedded atom model for iron and nickel in molecular dynamics simulation, Russ. J. Phys. Chem. A 87 (4) (2013) 615–622.
[21] S. Chen, Y. Zhang, M. Lagi, S. Chong, P. Baglioni, F. Mallamace, Evidence of dynamic crossover phenomena in water and other glass-forming liquids: experiments, md simulations and theory, J. Phys. Condens. Matter 21 (50) (2009) 504102.
[22] A. Korobov, Scaling properties of the area distribution functions and kinetic curves of dense plane discrete Poisson–Voronoi tessellations, Phys. Rev. E 87 (1) (2013) 014401.
[23] A. Korobov, Scaling properties of planar discrete Poisson–Voronoi tessellations with von Neumann neighborhoods constructed according to the nucleation and growth mechanism, Phys. Rev. E 89 (3) (2014) 032405.
[24] M. Daw, M. Baskes, Semiempirical, quantum mechanical calculation of hydrogen embrittlement in metals, Phys. Rev. Lett. 50 (17) (1983) 1285–1288, http://dx.doi.org/10.1103/PhysRevLett.50.1285.
[25] X.-Y. Liu, W. Xu, S.M. Foiles, J.B. Adams, Atomistic studies of segregation and diffusion in Al–Cu grain boundaries, Appl. Phys. Lett. 72 (13) (1998) 1578, http://dx.doi.org/10.1063/1.121120.
[26] D. Rapaport, The Art of Molecular Dynamics Simulation, Cambridge University Press, 2004.
[27] S. Plimpton, Fast parallel algorithms for short-range molecular dynamics, J. Comput. Phys. 117 (1) (1995) 1–19.
[28] D. Turnbull, Formation of crystal nuclei in liquid metals, J. Appl. Phys. 21 (10) (1950) 1022, http://dx.doi.org/10.1063/1.1699435.
[29] H.L. Peng, M.Z. Li, W.H. Wang, C.-Z. Wang, K.M. Ho, Effect of local structures and atomic packing on glass forming ability in Cu_xZr_{100x} metallic glasses, Appl. Phys. Lett. 96 (2) (2010) 021901, http://dx.doi.org/10.1063/1.3282800.
[30] T. Schenk, D. Holland-Moritz, V. Simonet, R. Bellissent, D. Herlach, Icosahedral short-range order in deeply undercooled metallic melts, Phys. Rev. Lett. 89 (7) (2002) 075507, http://dx.doi.org/10.1103/PhysRevLett.89.075507.
[31] L. Huang, C.Z. Wang, S.G. Hao, M.J. Kramer, K.M. Ho, Atomic size and chemical effects on the local order of Zr_2M (M = Co, Ni, Cu, and Ag) binary liquids, Phys. Rev. B 81 (1) (2010) 014108, http://dx.doi.org/10.1103/PhysRevB.81.014108.
[32] K. Kelton, G. Lee, A. Gangopadhyay, R. Hyers, T. Rathz, J. Rogers, M. Robinson, D. Robinson, First X-ray scattering studies on electrostatically levitated metallic liquids: demonstrated influence of local icosahedral order on the nucleation barrier, Phys. Rev. Lett. 90 (19) (2003) 195504, http://dx.doi.org/10.1103/PhysRevLett.90.195504.
[33] G.W. Lee, A.K. Gangopadhyay, T.K. Croat, T.J. Rathz, R.W. Hyers, J.R. Rogers, K.F. Kelton, Link between liquid structure and the nucleation barrier for icosahedral quasicrystal, polytetrahedral, and simple crystalline phases in Ti-Zr-Ni alloys: verification of Frank's hypothesis, Phys. Rev. B 72 (17) (2005) 174107, http://dx.doi.org/10.1103/PhysRevB.72.174107).
[34] P. Steinhardt, D. Nelson, M. Ronchetti, Icosahedral bond orientational order in supercooled liquids, Phys. Rev. Lett. 47 (18) (1981) 1297–1300, http://dx.doi.org/10.1103/PhysRevLett.47.1297.
[35] W. Luo, H. Sheng, F. Alamgir, J. Bai, J. He, E. Ma, Icosahedral short-range order in amorphous alloys, Phys. Rev. Lett. 92 (14) (2004) 145502, http://dx.doi.org/10.1103/PhysRevLett.92.145502.
[36] H. Reichert, O. Klein, H. Dosch, M. Denk, V. Honkimäki, T. Lippmann, G. Reiter, Observation of five-fold local symmetry in liquid lead, Nature 408 (6814) (2000) 839–841, http://dx.doi.org/10.1038/35048537 (URL http://www.ncbi.nlm.nih.gov/pubmed/11130718).
[37] D. Faken, H. Jónsson, Systematic analysis of local atomic structure combined with 3D computer graphics, Comput. Mater. Sci. 2 (2) (1994) 279–286.
[38] T.V. Tropin, G. Schulz, J.W. Schmelzer, C. Schick, Heat capacity measurements and modeling of polystyrene glass transition in a wide range of cooling rates, J. Non-Cryst. Solids 409 (0) (2015) 63–75 http://dx.doi.org/10.1016/j.jnoncrysol.2014.11.001 (URL http://www.sciencedirect.com/science/article/pii/S002230931400547X).
[39] X. Guo, M. Potuzak, J.C. Mauro, D.C. Allan, T. Kiczenski, Y. Yue, Unified approach for determining the enthalpic fictive temperature of glasses with arbitrary thermal history, J. Non-Cryst. Solids 357 (16–17) (2011) 3230–3236, http://dx.doi.org/10.1016/j.jnoncrysol.2011.05.014 (URL http://linkinghub.elsevier.com/retrieve/pii/S0022309311003607).
[40] S. Zhurkov, B. Levin, Investigations of the heat capacity of polymers in the solidification range, AN SSSR, 1950 260.
[41] H.B. Ke, P. Wen, W.H. Wang, The inquiry of liquids and glass transition by heat capacity, AIP Adv. 2 (4) (2012) 041404.
[42] G. Bartenev, Dokl. Akad. Nayk SSSR 76 (2) (1951) 226.
[43] M. Volkenstein, O. Ptizyn, Dokl. Akad. Nayk SSSR 103 (5) (1955) 795.
[44] M. Volkenstein, O. Ptizyn, Zh. Tekh. Fiz. 26 (10) (1956) 2204.
[45] V. Wessels, A.K. Gangopadhyay, K.K. Sahu, R.W. Hyers, S.M. Canepari, J.R. Rogers, M.J. Kramer, A.I. Goldman, D. Robinson, J.W. Lee, J.R. Morris, K.F. Kelton, Rapid chemical and topological ordering in supercooled liquid $Cu_{46}Zr_{54}$, Phys. Rev. B 83 (2011) 094116, http://dx.doi.org/10.1103/PhysRevB.83.094116.
[46] A. Takeuchi, A. Inoue, Quantitative evaluation of critical cooling rate for metallic glasses, Mater. Sci. Eng. A 304–306 (2001) 446–451 (rQ10, Tenth International Conference on Rapidly Quenched and Metastable Materials) http://dx.doi.org/10.1016/S0921-5093(00)01446-5. (URL http://www.sciencedirect.com/science/article/pii/S0921509300014465).